



**Acoustics'08
Paris**
June 29-July 4, 2008

www.acoustics08-paris.org

euonoise

Vortex sound of the flute and its interpretation

Andreas Bamberger

Physics Institute University Freiburg, Hermann-Herder-Str. 3, 79104 Freiburg, Germany
bamberger@physik.uni-freiburg.de

The flute as an example of flue instruments is investigated for its properties of the jet-labium interaction at 1kHz. The jet and the externally excited acoustic flow in the embouchure especially near the labium is recorded with endoscopic Particle-Image-Velocimetry. The data allows to calculate the vortex sound according to M. Howe (1975) by extracting the vorticity. The far field acoustic power of the flute is measured as well and compared with the vortex sound power which matches in sign and magnitude up to a factor 2 for different sound levels. The non-trivial interpretation of the sound production is based on the near cancellation of the two vortex layers of the jet along its path except near the labium. In order to gain insight of the interplay of the different ingredients of the vortex sound power the Coriolis force, the acoustic field and their phase relation are determined. A comparison with recently available numerical simulations (ISMA 2007) is discussed.

1 Introduction

The acoustic property of the flute has been investigated by N. Fletcher [1] and J. W. Coltman [2] with respect to the sound production mechanism. Basically the driving force for the excitation of the standing wave of the resonator is considered to be either the volume flow model of the jet resulting in the momentum transfer in the flute's body [1] or by the momentum transfer through the pressure difference in the region of the labium [2]. In the paper of M. Howe [4] the radiation of sound is described by the vortex sound term based on earlier publications by A. Powell [3]. Essentially the laminar jet develops an instability which leads to exponentially increasing transverse excursions between the flue formed by the lips and the labium. The interaction of the jet with the acoustic field near labium is described as a vortex convecting towards the labium and experiencing a Coriolis force. The presence of an acoustic field leads to a power delivering energy to or absorbing energy from the radiation field.

With the advent of the PIV a detailed measurement of the jet becomes feasible. Especially in the spatially constrained situation within the chimney of the embouchure the endoscopic PIV allows precise measurements of the vorticity. The measurement of the acoustic field in a standalone experiment completes the data in order to derive the power of the source term. In spite of idealising assumptions the power of radiation can be related quantitatively with the source term.

The aim of this contribution is the measurement of the phase shift between the Coriolis force and the acoustic field as a function of the jet speed.

2 Experimental setup

The flute is operated through an artificial mouth formed of silicon cautchouc with a flue inserted between the lips, see Fig. 1. The opening is chosen for normal operation of the flute to be $0.9\text{mm} \cdot 9.5\text{mm}$. Compressed air is loaded with $\sim 10\mu$ diameter droplets for the visualisation. The blowing pressure in the mouth is measured with a pressure gauge.

The PIV system is composed of a twin head NdYAG laser, a double exposure video camera and a timing control. The endoscope of 4mm in diameter is inserted into the chimney of the embouchure. The first lens of the optics is positioned flush to the blow hole. The optics is attached through an adapter onto the lens system of the video camera. The fish eye type of picture covers the flue

exit and the area near the labium which is positioned at a distance of about 5mm from the flue. This way the flow near the upper surface of the labium as well as near the lower surface of the edge can be recorded.

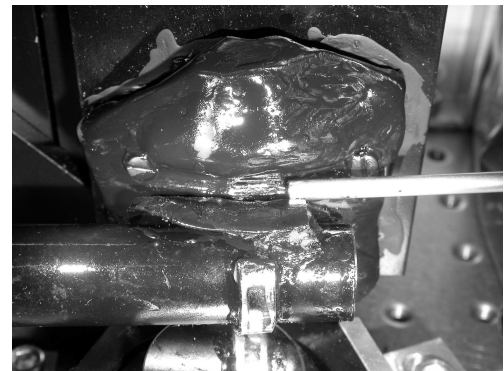


Figure 1: *View of the embouchure along the laser light direction. The light sheet illuminates the vertically the center of the flue-embouchure system. The endoscope optics is positioned on the right side about 5mm from the center. At the bottom a mirror reflects the laser light through a window on the flute head onto the region below the labium.*

The flute body is replaced by a polymer substitute essentially to ease the external excitation of the standing wave for the measurement of the acoustic field in the embouchure. The reference microphone is inserted at the position of the *Gi*s key as a timing trigger and for the absolute pressure p_{res} measurement of the standing wave. The excitation of the acoustic wave in the resonator is created with a sine-wave generator and a speaker-exponential horn system weakly coupled to the flute body. The horn remains for all the measurements, it barely affects the impedance of the resonator. The flute is operated at d3 with 1150 Hz. For the range of operation the content of higher harmonics is sufficiently small.

A box shaped confinement volume with transparent plastic foils serves for the homogenization of the seeding. The light sheet of the lasers is perpendicular to the flute axis. The laser pair is triggered by the microphone with pulse distances of $2\mu\text{s}$ for the jet velocity field, and of 5 to $10\mu\text{s}$ for the acoustic field. A part of the light sheet is reflected on a bottom mirror via a glass windows into the interior of the flute head illuminating the area below the labium.

3 Data taking

The data taking is triggered at a chosen phase, 16 per period of 870 μs for typically five shots. The phase is changed through the delay of 1/16 of the period. The evaluation is done with the VidPIV acquisition program. The correlation is evaluated in overlapping pixel areas corresponding to an interrogation area of $32 \cdot 32$ pixels. The displacement is 16 pixels producing a halfway overlap with the neighbouring interrogation areas. The resulting distance of the interrogation areas corresponds to $\approx 0.25 \text{ mm}$. For the measurement of the acoustic wave the air flow with the seeding was switched off during the exposure.

The mouth - embouchure geometry is adjustable in this experiment. The distance between the flue exit and the labium and the transverse displacement is steered by micrometer screws. The angle of attack can be chosen by the rotation of the flute around its axis. Moreover the coverage of the blow hole has to be about 40 - 50%. By changing the blowing pressure the flutist optimizes the efficiency and the tone quality by changing the geometry. In this scan however going from low to high blowing pressure it was tried to avoid unwanted systematics. Therefore the setting of the geometry was not changed.

The values for the operation of the flute for the data set and the main results are given in Table 1. The first column lists the maximum value of the jet speed determined by the PIV. The second column is the calculated power delivered to the system by the jet. The third column is the pressure in the resonator measured by the calibrated microphone, in order to relate the free field measurement with the actual condition. In the 5th column the free field power is quoted.

V_j [$\frac{m}{s}$]	P_j [mW]	p_{res} [Pa]	$P_{vor} > 0$ [mW]	P_{free} [mW]	$\frac{P_{vor}}{P_{free}}$
19	25 \pm 3	50 \pm 3	0.18 \pm 0.01	0.10 \pm 0.01	1.84
20	29 \pm 4	67 \pm 4	0.21 \pm 0.01	0.18 \pm 0,02	1.14
22	39 \pm 5	93 \pm 5	0.58 \pm 0.02	0.35 \pm 0.04	1.65
26	64 \pm 9	126 \pm 7	1.29 \pm 0.04	0.64 \pm 0.07	2.02
28	76 \pm 11	140 \pm 8	1.61 \pm 0.05	0.78 \pm 0.09	2.05

Table 1: Average values of flute operation and the results

4 Evaluation of the data and evaluation of the vortex sound power

The velocity field is displayed for a jet velocity of 22m/s in Fig. 2, upper part. The lips with the flue are at right border, above the jet is outside and below inside the flute. The shape of the labium seen as a wedge at the upper part. At this speed the jet is mostly laminar. At a finite thickness of the jet two shear layers of opposite vorticity $\vec{\omega}$ are formed, see Fig. 3, upper part. The curvature of the oscillating jet changes for upwards moving jet and downwards moving jet. This in turn affects the net vorticity as a function of time within a period if the spatial integration is done. Note that at this phase the

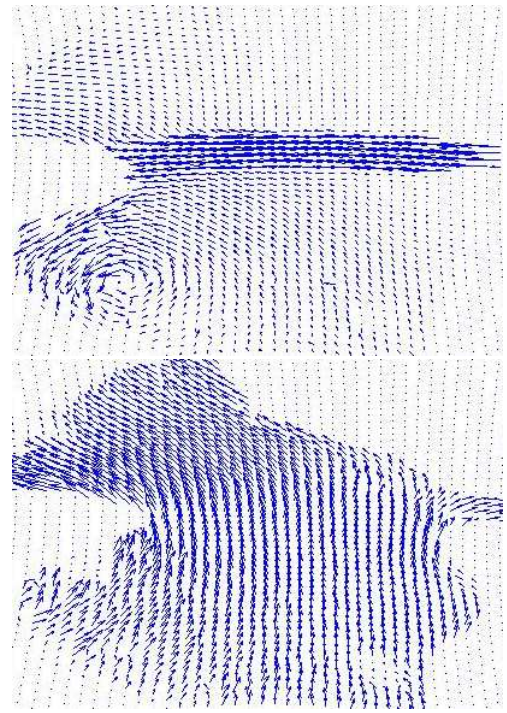


Figure 2: Upper part: Velocity field of the flute at 1150Hz and jet velocity of 22m/s. The jet is moving up. Lower part: Acoustic field, the arrows are scaled up for clarity.

vortex shedding is observed at the lower left corner inside the flute below the labium as it is the case for the outside half a period later.

For the following discussion the main component of the source term according to M. Howe [4] is needed:

$$\vec{f}_{cor} = -\rho_{air}(\vec{\omega} \times \vec{U}_{jet}). \quad (1)$$

with the Coriolis force density \vec{f}_{cor} , the density of air ρ_{air} and the vorticity $\vec{\omega}$. The vector $\rho_{air}(\vec{\omega} \times \vec{U}_{jet})$ is plotted on top of the vorticity. Its main component is vertical as can be seen.

In the following the acoustic field \vec{v}_{ac} is the second important factor. It is displayed for the same phase in Fig. 2, lower part. The field is dominantly vertical through all phases at the region covered by the jet.

According to Howe the instantaneous power density is proportional to $\vec{f}_{cor} \cdot \vec{v}_{ac}$. The integral over the volume of the embouchure will result in an instantaneous power. Note that the different parts of the jet, especially upper and lower shear layer are added here coherently.

Finally the power is averaged over one cycle and yields the total power:

$$P_{vort} = 1/T \int (\vec{f}_{cor} \cdot \vec{v}_{ac}) dV dt. \quad (2)$$

The integrand, namely the power density is displayed in Fig. 3, lower part. The integration results in a positive net power in the region near the labium. For a phase 180° apart there is a positive curvature of the jet, therefore the net vorticity and the net Coriolis force switches the sign, as well as the acoustic field: The integration results again in a positive value. Within the period of

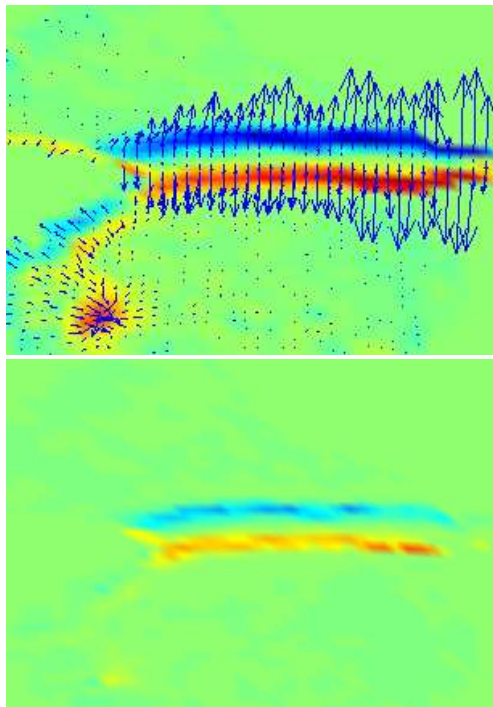


Figure 3: *Upper part: Vorticity of the jet in a rainbow colour code (blue = negative, red positive; the upper layer is here negative, the lower layer is positive) and the Coriolis force visualised as superimposed arrows. Lower part: The power density as a product of the Coriolis force and acoustic field (the upper layer is negative also). The net power is positive at this phase.*

870 μs the double peak structure of the instantaneous power. This corresponds to a push-pull action in a quasi symmetric configuration of the labium-jet system.

For the power evaluation the measured effective span-wise extension of the jet of 6 mm in (2) is used. We take the convention that a positive net power of the system delivers acoustic energy. Coherency is the main reason for the small efficiency of the free field power of the order of few percent of the input power. It obvious to compare this quantity with the free field acoustic power of the flute taken at the same reference pressure. There is an agreement within a factor two, see column 8 of Tab. 1.

Considering an integration area larger than the jet thickness there is a net vorticity, which changes the sign twice within a period. Considering for this reasoning the vertical components only, the scalar product of the net Coriolis force and the acoustical field may be positive or negative depending in general on the phase shift between the two quantities. For the flute it turns out that the product is predominantly positive over the period T , see [6, 7]. In order to evaluate the phase shift the Coriolis force may be approximated by the fundamental as it is done for the acoustic field.

It is interesting to determine the phase and the phase shift as the power is increased.

5 Evaluation of phase relationship between position of the jet, the Coriolis force with respect to the acoustic field

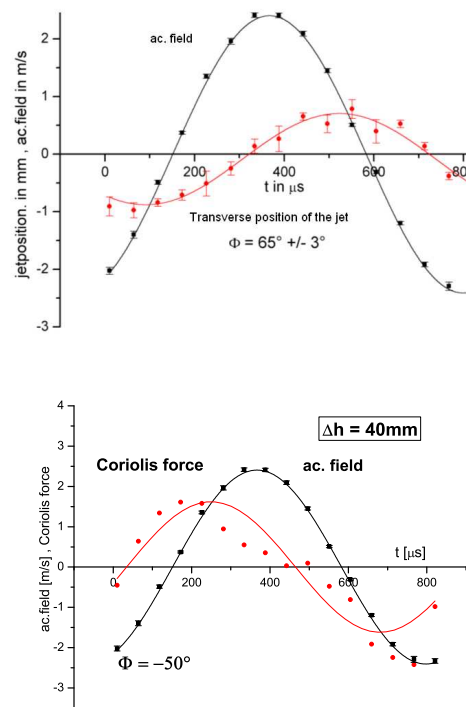


Figure 4: *Upper part: The phase shift as between the transverse jet position and the acoustic phase. Lower part: The integrated Coriolis force density (vertical component) in the same region and the acoustic field.*

In the following the plot of the position of the jet and the net Coriolis force as function of the time within a period is investigated. In Fig. 4 the phase determination is done by fitting the fundamental to the above quantities and the acoustic field. The phase difference is Φ is based on the definition that the acoustic field is fit with $\propto \sin(\omega t + \Phi)$. $\Phi < 0$ means a trailing acoustic field, $\Phi > 0$ the acoustic wave is advanced with respect to the quantity investigated. The vertical position of the jet is readily available from the data. As can be seen the acoustic phase is $+65 \pm 3^\circ$. For comparison with simulations and in order to be conform with definition of the phase shift of the jet position with the negative displacement of the acoustic field the phase is converted.

In the light of the underlying physics other quantities are more appropriate. This is done by fitting the fundamental onto to the Coriolis force which are integrated over an area just in front of the labium, where most of the power is produced, see the Fig. 4, lower part. Here the acoustic field is trailing by about -50° . In Tab. 2 the phase is given for the position of the jet in the 4th column, the converted angle with respect to the acoustic displacement in the 5th column and for the Coriolis force in the 6th column at different jet speeds.

A plot of the converted angle of the jet position with respect to the negative acoustic displacement is shown in

Fig. 6, upper part. Here the continuous line shows a fit to simulated data [8]. The data show a fair agreement.

In order to quantify the trend a plot of the phase shift as a function of the measured vortex power is made. A seemingly linear behaviour is fit by a straight line, see as an example the coriolis force in Fig. 5, upper part. The slope is about $-22^\circ/mW$. A similar slopes is observed in the case of jet position, see Tab. 2, bottom row. This is a sizable effect at a dynamic range of the power of almost one order of magnitude. Since it starts at low power already with an offset of -25° one might think that the effect gives rise to a saturation of the source term beyond 2 mW.

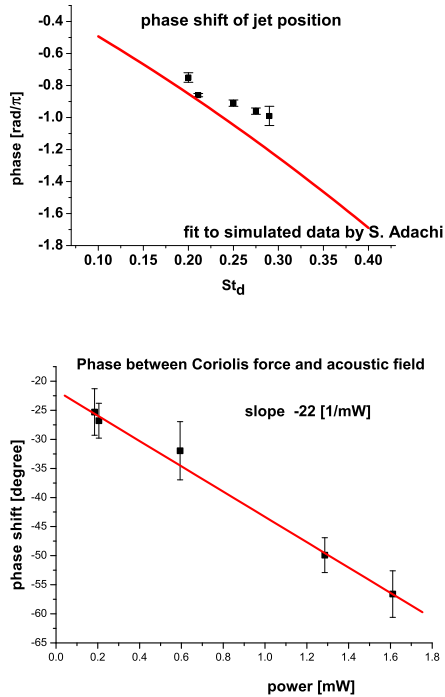


Figure 5: *Upper part: Phase shift of the jet position with respect to the negative displacement of the acoustic field, see [8]. Lower part: Phase shift of the Coriolis force as a function of the power.*

V_{jet} [$\frac{m}{s}$]	Str_d	P_{vor} [mW]	Φ_{pos-ac} [$^\circ$]	Φ_{ad-pos} [rad/ π]	$\Phi_{corf-ac}$ [$^\circ$]
19	0.30	0.184	$+88 \pm 11$	-0.99 ± 0.06	-25 ± 4
20	0.29	0.205	$+82 \pm 4$	-0.96 ± 0.02	-27 ± 3
22	0.26	0.58	$+73 \pm 3$	-0.91 ± 0.02	-32 ± 5
26	0.22	1.29	$+65 \pm 2$	-0.86 ± 0.01	-50 ± 3
27.5	0.21	1.61	$+46 \pm 5$	-0.75 ± 0.03	-57 ± 4
$d\Phi/dP$			-19 ± 3		-22 ± 3

Table 2: *Phase of flute operation at different jet speeds. The Strouhal number $Str_d = fd/U_{jet}$, the power P_{vort} , the phase shift and slope of the respective quantity are listed.*

6 The vortex sound and its interpretation

The determination of acoustic sources is carried out with the scalar product of the coriolis force and the acoustic field. Since the wave length of the acoustic field (~ 0.3 m) is much larger than the integration volume (1 cm^3) the phases of the contributing elements matter. This corresponds to a coherence situation often encountered in the physics of radiation. For flutes, and supposedly for many flue instruments in general, one encounters shear layers of opposite vorticity next to each other and therefore produce a near cancellation after integration of the relevant volume. In the case of the flute, at least for the investigated regime of operation, the difference of the power density of the shear layers is orders of magnitude larger than the net power after integration. As a result the vortex sound power is two orders of magnitude smaller than the power delivered to the system by the jet.

Consideration for vortex sound power.

1. As can be shown by converting a double cross product into a sum of scalar products the coriolis force expression can be cast into a pressure difference across the jet which delivers work by the displacement in the acoustic field per unit time. This might serve as an alternative interpretation of the vortex sound power. This explanation is commonly alluded to the Magnus effect in textbooks.
 2. Having an energy producing mechanism near the flue it would have to be added to the excitation of the standing wave of the resonator. Since the quantity is much smaller than the energy transferred as the jet enters into the pipe, the total power balance is not really affected in the regime investigated here.
 3. The discrepancy of a factor ~ 2 between the vortex power and the free field power has two aspects.
 - The acoustic field at the embouchure in this experiment was checked for its content of vorticity. It was found to be small.
- However there might be a yet undetected vortex of energy absorbing nature at a scale length not accessible with the present setup. Indeed the spatial resolution is limited by the investigation area to about 0.2 mm. This is especially true at the borders of the labium. Through convection of such an object drifts away from the borders, it would become eventually visible. Notwithstanding it would be integrated over for the final result on this part of its trajectory.
- There is of course still a radiation contribution from the end correction of the standing wave leaking into the free space at the open end of the resonator. This would be also considered as a coherent source.
 4. Such power absorbing processes by vortices in tubes are known from the literature [9, 10]. They are

called nonlinear terms of interaction with the radiation field. More recent investigations by D. Skulina are confirming these results to great extent [11]. This allows an estimate of the contribution also for this experiment. Taking the ratio of the impedances Z_{nl} normalized by Z_c of the tube a general dependence may be cast into the following form

$$Z_{nl}/Z_c = \beta \cdot M \cdot (St'_d)^{1/3} \quad (3)$$

with β between 0.6 and 1.0, the Mach number u_{ac}/c and St'_d as a function of u_{ac} . Taking the acoustic amplitudes in this experiment ranging between 0.9 and 2.5 m/s this quantity amounts to be <0.01 . This seems to be on the safe side, however it should be mentioned that there is a flow transition observed at about 2 m/s [11].

7 Summary

In summary it can be stated that

- The power determination of the flute through the vortex sound sources are at low to moderate sound pressure levels close to the free field radiation power within a factor ~ 2 .
- At this stage of investigation a sizable modification of this ratio due to nonlinear effects seems to be unlikely.

References

- [1] M. Fletcher, N. H., J. Acoust. Soc. Am., Vol. 60, p. 481, 1976
- [2] Coltman, J.W., J. Acoust. Soc. Am., Vol. 44, p. 983, 1968
- [3] Powell, A., J. Acoust. Soc. Am., Vol. 36, p. 177, 1964
- [4] Howe, M. S., Fluid. Mech., Vol. 71, p. 625, 1975
- [6] Bamberger, A., Forum Acusticum Budapest 2005, 4th European Congress on Acoustics : 29 August - 2 September 2005
- [7] Bamberger, A., Vortex Sound of the Flute, ISMA2007, Barcelona, 9 - 12th September
- [8] S. Adachi et al., Numerical Simulation of an Air Jet and Modeling of its Deflection by Sound, ISMA2007, Barcelona, 9 - 12th September
- [9] Disselhorst, J.H.M. and Van Vijngaarden, L. (1980). Flow in the exit of open pipes during acoustic resonance, J. Fluid Mech. 99(2), pp. 293-319
- [10] Fabre, B., Hirschberg, A. and Wijnands, A.P.J. (1996). Vortex shedding in steady oscillations of a flue organ pipe, Acustica 82, pp. 863-877
- [11] D. J. Skulina, A Study of Non-linear Acoustic Flows at the open end of a Tube using Particle Image Velocimetry, PhD Thesis, University of Edinburgh 2005